

MHD MICROPOLAR FLUID FLOW TOWARDS A VERTICAL SURFACE IN PRESENCE OF HEAT SOURCE/SINK UNDER RADIATIVE HEAT FLUX

A. Adhikari and A.K.Maiti

ABSTRACT. A steady two-dimensional incompressible magnetohydrodynamics micropolar fluid flow towards a stretching or shrinking vertical sheet under suction or blowing with prescribed surface heat flux is studied in this paper. The transport equations employed in the analysis include the effect of radiative heat flux under mixed convection. Similarity transformation is used to convert the governing non-linear boundary-layer equations to coupled higher order nonlinear ordinary differential equation. These transformed differential equations are solved numerically by a finite-difference scheme, known as Keller-box method. Numerical results are obtained for the velocity, microrotation and temperature distributions, as well as the skin friction coefficient and local Nusselt number for various parameters and then these are shown graphically. Dual similarity solutions are found to exist for the opposing flow, while for the assisting flow, the solution is unique. Suction, applied magnetic field and micropolar fluids delay the boundary-layer separation and exhibit drag reduction as compared to the non-suction, non-magnetic field and classical Newtonian fluid respectively. The present results are compared with available results in literature and found a good agreement with them.

1. Introduction

The study of stagnation point flow towards a solid surface in moving fluid traced back to Hiemenz in 1911. He was the pioneer to analyze two-dimensional stagnation-point flow on stationary plate using a similarity transformation to reduce

2010 *Mathematics Subject Classification.* 76W05, 76S05.

Key words and phrases. Heat generation/absorption, micropolar fluid, radiative heat flux, similarity transformations, Keller-box method.

The authors gratefully acknowledge the financial support received from the UGC, INDIA (Minor Research Project: PSW 145/11-12 (ERO) 25 Jan 12) and are also thankful to the referee for the constructive suggestions and useful comments to improve the paper .

the Navier-Stokes equations to non-linear ordinary differential equations. Since then many investigators have extended the idea to different aspect of the stagnation-point flow problems in various way. Accordingly, Mahapatra and Gupta [1] numerically analyzed two-dimensional boundary-layer flow, stagnation-point flow and heat transfer over a stretching sheet. Wang [2] studied two-dimensional stagnation-point flow on stretching sheet and on axisymmetric shrinking sheet. Lok et al. [3] observed non-orthogonal stagnation-point flow towards a shrinking sheet. It was found that the obliqueness of a free stream line causes the shifting of the stagnation-point towards the incoming flow.

Laminar boundary layer behavior over a moving continuous and linearly stretching surface is a significant type of flow has considerable practical applications in engineering and polymer processing. For example, materials manufactured by extrusion processes and heat treated materials traveling between a feed roll and a windup roll or on a conveyor belt possess the characteristics of a moving continuous surface. The hydromagnetic flow and heat transfer problems have become important industrially. To be more specific, it may be pointed out that many metallurgical processes involve the cooling of continuous strips or filaments by drawing them through a quiescent fluid and that in the process of drawing, these strips are sometimes stretched. Mention may be made of drawing, annealing and tinning of copper wires. In all the cases the properties of the final product depend to a great extent on the rate of cooling. By drawing such strips in an electrically conducting fluid subjected to a magnetic field, the rate of cooling can be controlled and a final product of desired characteristics can be achieved. Another interesting application of hydromagnetics to metallurgy lies in the purification of molten metals from nonmetallic inclusions by the application of a magnetic field. The study of heat and mass transfer is necessary for determining the quality of the final product. The significant work in this area was conducted by Sakiadis [4, 5, 6]. He analyzed the boundary layer assumptions and the governing equations of the problem on a continuously stretching surface with a constant velocity. Thermal radiation effects could play an important role in controlling heat transfer in industry. Heat transfer characteristics of a continuous stretching surface with variable temperature were studied by Grubka and Bobba [7]. Cortwell [8] discussed the effects of viscous dissipation and radiation on the thermal boundary layer over a non-linearly stretching sheet. Spreiter and Rizzi [9] studied in the context of solar wind radiative magnetohydrodynamics. Nath et al. [10] obtained a set of similarity solutions for radiative MHD steller point explosion dynamics using shooting methods. Chen [11] studied the effects of anisotropic scattering on steady non-similar free convective radiative hydromagnetic boundary layer flow over a diffuse reflecting surface solving a separate equation for magnetic field distribution. Noor et al. [12] studied the effect of heat source/sink on MHD free convection thermophoretic flow over a radiative isothermal inclined plate. Most recently, heat transfer problems for boundary layer flow concerning a convective boundary condition was investigated by Aziz [13] for the Blasius flow. Similar analysis was applied to the Blasius and Sakiadis flow with radiation effect by Bataller [14]. Makinde [15, 16] studied the heat and mass transfer over a vertical plate with convective boundary conditions.

The theory of microrotation fluids, first studied by Eringen [17], display the effects of local rotary inertia and couple stresses, can explain the flow behavior due to the microscopic effects arising from the local structure and micromotions of the fluid elements in which the classical Newtonian fluids theory is inadequate. These fluids contain dilute suspensions of rigid micromolecules with individual motions which support stress and body moments and influenced by spin-inertia. The extension of the theory of micropolar to thermomicropolar fluids was also investigated by Eringen [18]. He established a suitable non-Newtonian fluid models which could be used to analyze the behavior of exotic lubricants (Khonsari [19]), polymeric fluids (Hadimoto [20]), liquid crystals (Lee et al. [21]), paints, animal blood (Ariman et al. [22]), colloidal suspensions, ferro-liquids etc. Kolpashchikov et al. [23] have derived a method to measure micropolar parameters experimentally. A thorough review of this subject and application of micropolar fluid mechanics has been provided by Ariman et al. [24]. Studies of the flow of heat convection in micropolar fluids have been focused on flat plate by Yucel [25], Jena and Mathur [26], Gorla [27], Hossain et al. [28] and Mori [29] etc. Several researchers have investigated the theory and its applications such as Lukaszewicz [30], Eringen [31] etc.

The stagnation-point flow of a micropolar fluid towards a stretching sheet was studied by Nazar et al. [32]. Similarly Ishak et al. [33] investigated stagnation-point flow over a shrinking sheet in a micropolar fluid and established that the solution is different from a stretching sheet. It was found that the solutions for a shrinking sheet are not unique. Furthermore, Ishak et al. [34] analyzed a mixed stagnation-point flow of a micropolar fluid towards a stretching sheet. Hayat et al. [35] discussed the MHD flow of a micropolar fluid near a stagnation-point towards a non-linear stretching surface. Further, Nadeem et al. [36] extended the problem to porous medium. Ashraf and Ashraf [37] incorporated the heat transfer parameter to stagnation-point flow. Ali et al. [38] included the idea of induced magnetic field to the problem of Ashraf. Moreover, Hayat et al. [39] investigated stagnation-point flow of a Maxwell fluid with magnetic field and radiation effect. Laminar mixed convection in two-dimensional stagnation flows around heated surfaces in the case of arbitrary surface temperature and heat flux variations was examined by Ramachandran et al. [40]. They established a reverse flow developed in the buoyancy opposing flow region and dual solutions are found to exist for a certain range of the buoyancy parameter. Devi et al. [41] extended this work for unsteady case. Lok et al. [42] studied the case for a vertical surface immersed in a micropolar fluid. Mahapatra and Gupta [43] studied the MHD stagnation point flow over a stretching surface. Chen [44] considered the combined effects of Joule heating and viscous dissipation on MHD flow past a permeable stretching surface with free convection and radiative heat transfer. Chin et al. [45], Ling et al. [46] and Ishak et al. [47] reported the existence of dual solutions in the opposing flow case. Hydromagnetic thermal boundary layer flow of a perfectly conducting fluid observed by Das [48]. Mukhopadhyay et al. [49] discussed Lie group analysis of MHD boundary layer slip flow past a heated stretching sheet in presence of heat source/sink. Shit and Halder [50] examined thermal radiation effects on MHD viscoelastic fluid flow over a stretching sheet with variable viscosity. Heat transfer

effects on MHD viscous flow over a stretching sheet with prescribed surface heat flux is studied by Adhikari and Sanyal [51]. Adhikari [52] also studied on MHD micropolar fluid flow towards a stagnation point on a vertical surface under induced magnetic field with radiative heat flux. The study of boundary layer flow against a vertical surface problem was considered by Cramer [53], Cobble [54], Raptis et al. [55], Kumari et al. [56] and so many researchers. Recently, Bachok and Ishak [57] studied MHD stagnation-point flow of a micropolar fluid with prescribed wall heat flux the vertical plate.

The aim of this paper is to make a numerical calculation, on mixed convective heat transfer flow which have been of interest to the engineering community and to the investigators dealing with the problem in geophysics, astrophysics and polymer processing. From the technical point of view mixed convection flow past an infinite vertical plate is always important for many practical applications. In this paper, we have considered a two-dimensional steady MHD mixed convection stagnation point flow of an incompressible micropolar fluid towards a stretching vertical surface with prescribed surface heat flux together with the effect of radiative heat flux under uniform transverse magnetic field which is normal to the surface.

2. Basic Equations

Consider a steady, two-dimensional flow of an incompressible electrically conducting micropolar fluid toward a stagnation point past a vertical plate with prescribed surface heat flux. The frame of reference (x,y) is chosen such that the x -axis is along the direction of the surface and the y -axis is normal to the surface, as shown in Fig.1. It is assumed that the velocity of the flow external to the boundary layer $U(= ax)$ and the surface heat flux $q_w(x)(= bx)$, temperature $T_w(x)$ of the plate are proportional to the distance x from the stagnation point, where a, b are constants. A uniform magnetic field of strength B_0 is assumed to be applied in the positive y -direction, normal to the vertical plate. The assisting flow situation occurs if the upper half of the flat surface is heated while the lower half of the flat surface is cooled. In this case the flow near the heated flat surface tends to move upward and the flow near the cooled flat surface tends to move downward. So this behaviour acts to assist the flow field. The opposing flow situation occurs if the upper half of the flat surface is cooled while the lower half of the flat surface is heated. The governing equations are

$$(1) \quad \frac{\partial u}{\partial x} + \frac{\partial v}{\partial y} = 0,$$

$$(2) \quad u \frac{\partial u}{\partial x} + v \frac{\partial u}{\partial y} = U \frac{dU}{dx} + \left(\frac{\mu + \kappa}{\rho} \right) \frac{\partial^2 u}{\partial y^2} + \frac{\kappa}{\rho} \frac{\partial N}{\partial y} + \frac{\sigma B_0^2}{\rho} (U - u) + g\beta(T - T_\infty),$$

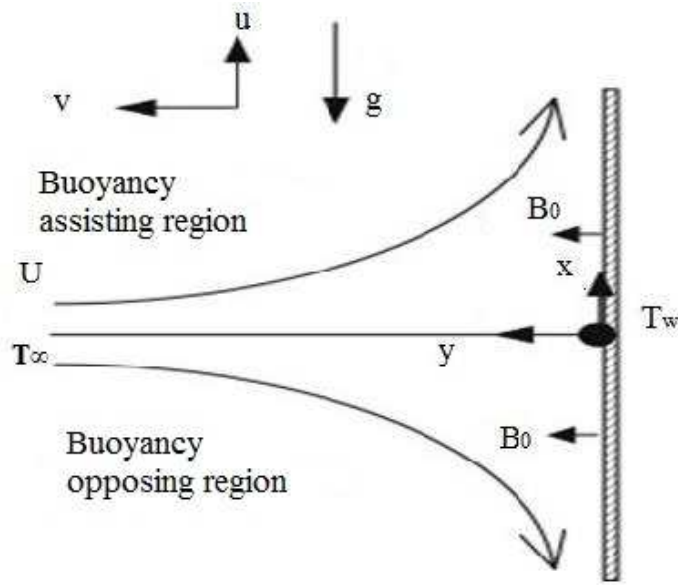


FIGURE 1. Model of the problem

$$(3) \quad \rho j \left(u \frac{\partial N}{\partial x} + v \frac{\partial N}{\partial y} \right) = \gamma \frac{\partial^2 N}{\partial y^2} - \kappa \left(2N + \frac{\partial u}{\partial y} \right),$$

$$(4) \quad u \frac{\partial T}{\partial x} + v \frac{\partial T}{\partial y} = \alpha \frac{\partial^2 T}{\partial y^2} - \frac{1}{\rho C_p} \frac{\partial q_r}{\partial y}.$$

The boundary conditions are
at $y = 0$:

$$(5) \quad \begin{aligned} u &= u_w(x) = cx, & v &= v_w(x), \\ N &= -n \frac{\partial u}{\partial y}, & \frac{\partial T}{\partial y} &= -\frac{q_w}{k}, \end{aligned}$$

at $y = \infty$:

$$(6) \quad u \rightarrow U = ax, \quad N \rightarrow 0, \quad T \rightarrow T_\infty.$$

where u and v are the velocity components along the x and y -axis respectively, $u_w(x)$ the wall shrinking or stretching velocity ($c > 0$ for stretching, $c < 0$ for shrinking and $c = 0$ for static wall), $v_w(x)$ the wall mass flux velocity, N is the microrotation or angular velocity whose direction of rotation is in the xy plane,

$\mu(= \nu\rho)$ is the dynamic viscosity, ρ is the density of the fluid, ν is the coefficient of viscosity, σ is the electrical conductivity, j is the micro-inertia per unit mass, i.e., micro-inertia density, γ is the spin gradient viscosity, κ is the vortex viscosity or micro-rotation viscosity, T is the fluid temperature in the boundary layer, T_∞ is the uniform ambient temperature, β is the thermal expansion coefficient, $\alpha(= \frac{k}{\rho C_p})$ is the thermal diffusivity, k is the thermal conductivity, q_w is the wall heat flux. Note that n is a constant such that $0 \leq n \leq 1$. When $n = 0$ then $N = 0$ at the wall represents concentrated particle flows in which the microelements close to the wall surface are unable to rotate. This case is also known as the strong concentration of microelements. When $n = 1/2$, we have the vanishing of anti-symmetric part of the stress tensor and denotes weak concentration of microelements, the case $n = 1$ is used for the modeling of turbulent boundary layer flows. We shall consider here both cases of $n = 0$ and $n = 1/2$. Assume $\gamma = (\mu + \kappa/2)j = \mu(1 + K/2)j$, where $K = \kappa/\mu$ is the micropolar or material parameter, $K \neq 0$ for micropolar fluid and $K = 0$ for the classical Newtonian fluid. This assumption is invoked to allow the field of equations that predicts the correct behavior in the limiting case when the microstructure effects become negligible and the total spin N reduces to the angular velocity (Ahmadi [58], Yucel [25]).

By using the Rosseland approximation the radiative heat flux q_r in y -direction is given by (Brewster [59])

$$(7) \quad q_r = -\frac{4\sigma_s}{3k_e} \frac{\partial T^4}{\partial y},$$

where σ_s is the Stefan-Boltzmann constant and k_e the mean absorption coefficient. It should be noted that by using Rosseland approximation, the present study is limited to optically thick fluids. Expanding T^4 in a Taylor series about T_∞ as:

$$(8) \quad T^4 = T_\infty^4 + 4T_\infty^3(T - T_\infty) + 6T_\infty^2(T - T_\infty)^2 + \dots,$$

and then neglecting higher order terms beyond the first degree in $(T - T_\infty)$, we get

$$(9) \quad T^4 = 4T_\infty^3 T - 3T_\infty^4,$$

In view of the equations (7) and (9), the equation (4) becomes

$$(10) \quad u \frac{\partial T}{\partial x} + v \frac{\partial T}{\partial y} = \alpha \frac{\partial^2 T}{\partial y^2} + \frac{16\sigma_s T_\infty^3}{3k_e \rho C_p} \frac{\partial^2 T}{\partial y^2}.$$

Introduce a Stream function ψ as follows

$$(11) \quad u = \frac{\partial \psi}{\partial y}, \quad v = -\frac{\partial \psi}{\partial x}.$$

The momentum, angular momentum and energy equations can be transformed into the corresponding ordinary differential equations by the following transformation:

$$(12) \quad \begin{aligned} \eta &= y\sqrt{a/\nu}, & f(\eta) &= \frac{\psi}{x\sqrt{a\nu}}, \\ p(\eta) &= \frac{N}{ax\sqrt{a/\nu}}, & \theta(\eta) &= \frac{k(T - T_\infty)}{q_w} \sqrt{a/\nu}, \end{aligned}$$

where η the independent dimensionless similarity variable. Thus u and v are given by $u = axf'(\eta)$, $v = -\sqrt{a\nu}f(\eta)$, Substituting variables (12) into equations (2), (3) and (10), we get the following ordinary differential equations:

$$(13) \quad (1 + K)f''' + ff'' + 1 - f'^2 + Kp' + M(1 - f') + \lambda\theta = 0,$$

$$(14) \quad (1 + K/2)p'' + fp' - pf' - K(2p + f'') = 0,$$

$$(15) \quad \frac{1}{P_r} \left(1 + \frac{4}{3F}\right) \theta'' + f\theta' - \theta f' = 0,$$

subject to the boundary conditions (5) and (6) which become

$$(16) \quad f(0) = s, \quad f'(0) = e, \quad p(0) = -nf''(0), \quad \theta'(0) = -1,$$

$$(17) \quad f'(\eta) \rightarrow 1, \quad p(\eta) \rightarrow 0, \quad \theta(\eta) \rightarrow 0, \quad \text{as } \eta \rightarrow \infty.$$

Here $f(\eta)$, $p(\eta)$ and $\theta(\eta)$ give (dimensionless) the velocity, the angular velocity and temperature respectively. In the above equations, primes denote differentiation with respect to η ; $j = \nu/a$ the characteristic length (Rees and Bassom [60]), $P_r = \nu/\alpha$ the Prandtl number, $M = \sigma B_0^2/(\rho a)$ the magnetic parameter, $e = c/a$ the velocity ratio parameter, $s = -v_w(x)/\sqrt{a\nu}$ the constant mass flux with $s > 0$ for suction and $s < 0$ for injection, $\lambda = Gr_x/Re_x^2$ the buoyancy or mixed convection parameter, $Gr_x = g\beta(T_w - T_\infty)x^3/\nu^2$ the local Grashof number, $Re_x = Ux/\nu$ is the local Reynolds number and $F = \frac{k_e k}{4\sigma_s T_\infty^3}$ the radiation parameter. Here λ is a constant and the negative and positive values of λ correspond to the opposing and assisting flows respectively. When $\lambda = 0$, i.e., when $T_w = T_\infty$ is for pure forced convection flow.

The skin friction coefficient C_f and the local Nusselt number Nu_x are defined as

$$(18) \quad C_f = \frac{\tau_w}{\rho U^2/2}, \quad Nu_x = \frac{xq_w}{k(T_w - T_\infty)}.$$

where the wall shear stress τ_w and the heat flux q_w are given by

$$(19) \quad \tau_w = \left[(\mu + \kappa) \frac{\partial u}{\partial y} + \kappa N \right]_{y=0}, \quad q_w = -k \left[\frac{\partial T}{\partial y} \right]_{y=0}.$$

with k being the thermal conductivity. Using the similarity variables (12), we get

$$(20) \quad \frac{1}{2}C_f Re_x^{1/2} = [1 + (1 - n)K/2] f''(0), \quad \frac{Nu_x}{Re_x^{1/2}} = \frac{1}{\theta(0)}.$$

3. Numerical Solutions

The equations(13), (14) and (15) subject to the boundary conditions(16) and (17) are solved numerically using an implicit finite-difference scheme known as the Keller-box method (Cebeci and Bradshaw [61], Cebeci and Cousteix [62] and Na [63]). The method has following four basic steps:

- (i) Reduce Equations(13) ,(14) and (15) to first order equations;
- (ii) Write the difference equations using central differences;
- (iii) Linearise the resulting algebraic equations by Newtons method and write them in Matrix-vector form;
- (iv) Use the Block-tridiagonal elimination technique to solve the linear system.

3.1. The Finite difference scheme. In this section, steps (i) and (ii) are combined. First we introduce new dependent variables $u(x, \eta), v(x, \eta), g(x, \eta)$ and $q(x, \eta)$ such that

$$(21) \quad f' = u, \quad u' = v, \quad p' = g, \quad \theta' = q,$$

so that equations (13),(14) and (15) reduce to

$$(22) \quad (1 + K)v' + fv + 1 - u^2 + Kg + M(1 - u) + \lambda\theta = 0,$$

$$(23) \quad (1 + K/2)g' + fg - pu - K(2p + v) = 0, .$$

$$(24) \quad \frac{1}{P_r} \left(1 + \frac{4}{3F}\right) q' + fq - u\theta = 0.$$

We now consider the net rectangle in the $x\eta$ plane as shown in fig.2 and the net points defined as follows:

$$(25) \quad x^0 = 0, \quad x^n = x^{n-1} + k_n, \quad n = 1, 2, \dots, N,$$

$$(26) \quad \eta_0 = 0, \quad \eta_j = \eta_{j-1} + h_j, \quad j = 1, 2, \dots, J, \quad \eta_J = \eta_\infty,$$

where k_n is the Δx - spacing and h_j is the $\Delta \eta$ - spacing. Here n and j are the sequence of numbers that indicate the coordinate location, not tensor indices or exponents.

Here we use the following finite-differences:

$$(27) \quad ()_{j-1/2}^n = \frac{1}{2}[()_j^n + ()_{j-1}^n],$$

$$(28) \quad ()_j^{n-1/2} = \frac{1}{2}[(\)_j^n + (\)_j^{n-1}],$$

$$(29) \quad \left(\frac{\partial u}{\partial x}\right)_{j-1/2}^{n-1/2} = \frac{[(u)_{j-1/2}^n - (u)_{j-1/2}^{n-1}]}{k_n},$$

$$(30) \quad \left(\frac{\partial u}{\partial \eta}\right)_{j-1/2}^{n-1/2} = \frac{[(u)_{j-1/2}^{n-1/2} - (u)_{j-1}^{n-1/2}]}{h_j},$$

Now we write the finite-difference for the midpoint $(x^n, \eta_{j-1/2})$ of the segment P_1P_2 using (27) to (30) . This process is called "centering about $(x^n, \eta_{j-1/2})$ ". We get by omitting upper indices n:

$$(31) \quad f_j - f_{j-1} - \frac{h_j}{2}(u_j + u_{j-1}) = 0,$$

$$(32) \quad u_j - u_{j-1} - \frac{h_j}{2}(v_j + v_{j-1}) = 0,$$

$$(33) \quad p_j - p_{j-1} - \frac{h_j}{2}(g_j + g_{j-1}) = 0,$$

$$(34) \quad \theta_j - \theta_{j-1} - \frac{h_j}{2}(q_j + q_{j-1}) = 0,$$

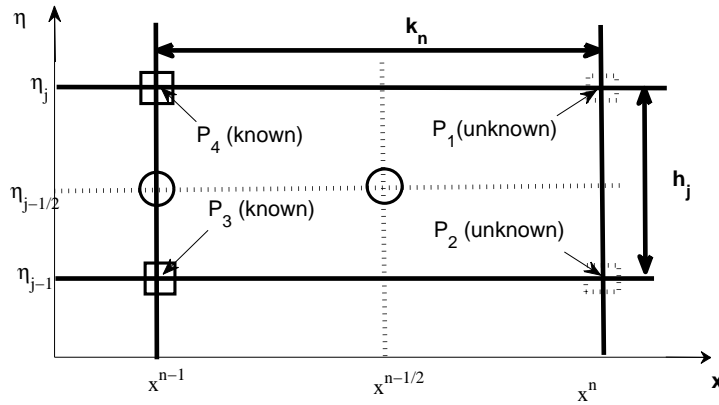


FIGURE 2. Net Rectangle for difference approximation

$$\begin{aligned}
(35) \quad & \frac{(1+K)}{h_j}(v_j - v_{j-1}) + \frac{1}{4}(f_j + f_{j-1})(v_j + v_{j-1}) \\
& + 1 - \frac{(u_j + u_{j-1})^2}{4} + \frac{K}{2}(g_j + g_{j-1}) \\
& + M \left[1 - \frac{(u_j + u_{j-1})}{2} \right] + \lambda \frac{(\theta_j + \theta_{j-1})}{2} = 0,
\end{aligned}$$

$$\begin{aligned}
(36) \quad & \left(1 + \frac{K}{2} \right) \frac{(g_j - g_{j-1})}{h_j} + \frac{1}{4}(f_j + f_{j-1})(g_j + g_{j-1}) \\
& - \frac{1}{4}(u_j + u_{j-1})(p_j + p_{j-1}) \\
& - K \left[(p_j + p_{j-1}) + \frac{(v_j + v_{j-1})}{2} \right] = 0,
\end{aligned}$$

$$\begin{aligned}
(37) \quad & \frac{(q_j - q_{j-1})}{P_r h_j} \left(1 + \frac{4}{3F} \right) + \frac{1}{4}(f_j + f_{j-1})(q_j + q_{j-1}) \\
& - \frac{1}{4}(u_j + u_{j-1})(\theta_j + \theta_{j-1}) = 0.
\end{aligned}$$

The boundary conditions at $x = x^N$ are

$$\begin{aligned}
(38) \quad & f_0^N = 0, \quad u_0^N = 0, \quad p_0^N = -nv_0^N, \\
& q_0^N = -1, \quad u_j^N = 1, \quad p_j^N = 0, \quad \theta_j^N = 0.
\end{aligned}$$

3.2. Newton's method for linearisation. To linearise the nonlinear system (31) to (37), we introduce the following i -th iterate at $x = x^n$:

$$\begin{aligned}
(39) \quad & f_j^{(i+1)} = f_j^{(i)} + \delta f_j^{(i)}, \quad u_j^{(i+1)} = u_j^{(i)} + \delta u_j^{(i)}, \\
& v_j^{(i+1)} = v_j^{(i)} + \delta v_j^{(i)}, \quad p_j^{(i+1)} = p_j^{(i)} + \delta p_j^{(i)}, \\
& g_j^{(i+1)} = g_j^{(i)} + \delta g_j^{(i)}, \quad \theta_j^{(i+1)} = \theta_j^{(i)} + \delta \theta_j^{(i)}, \\
& q_j^{(i+1)} = q_j^{(i)} + \delta q_j^{(i)}.
\end{aligned}$$

Substituting these in (31) to (37) and then retaining only the linear terms in $\delta f_j^{(i)}, \delta u_j^{(i)}, \delta v_j^{(i)}, \delta p_j^{(i)}, \delta g_j^{(i)}, \delta \theta_j^{(i)}$ and $\delta q_j^{(i)}$, we get the following linear tridiagonal system:

$$(40) \quad \delta f_j - \delta f_{j-1} - \frac{h_j}{2}(\delta u_j + \delta u_{j-1}) = (r_1)_j,$$

$$(41) \quad \delta u_j - \delta u_{j-1} - \frac{h_j}{2}(\delta v_j + \delta v_{j-1}) = (r_2)_j,$$

$$(42) \quad \delta p_j - \delta p_{j-1} - \frac{h_j}{2}(\delta g_j + \delta g_{j-1}) = (r_3)_j,$$

$$(43) \quad \delta \theta_j - \delta \theta_{j-1} - \frac{h_j}{2}(\delta q_j + \delta q_{j-1}) = (r_4)_j,$$

$$(44) \quad \begin{aligned} & (a_1)_j \delta f_j + (a_2)_j \delta f_{j-1} + (a_3)_j \delta u_j + (a_4)_j \delta u_{j-1} \\ & + (a_5)_j \delta v_j + (a_6)_j \delta v_{j-1} + (a_7)_j \delta g_j + (a_8)_j \delta g_{j-1} \\ & + (a_9)_j \delta \theta_j + (a_{10})_j \delta \theta_{j-1} = (r_5)_j, \end{aligned}$$

$$(45) \quad \begin{aligned} & (b_1)_j \delta f_j + (b_2)_j \delta f_{j-1} + (b_3)_j \delta u_j + (b_4)_j \delta u_{j-1} \\ & + (b_5)_j \delta v_j + (b_6)_j \delta v_{j-1} + (b_7)_j \delta p_j + (b_8)_j \delta p_{j-1} \\ & + (b_9)_j \delta g_j + (b_{10})_j \delta g_{j-1} = (r_6)_j, \end{aligned}$$

$$(46) \quad \begin{aligned} & (c_1)_j \delta f_j + (c_2)_j \delta f_{j-1} + (c_3)_j \delta u_j \\ & + (c_4)_j \delta u_{j-1} + (c_5)_j \delta \theta_j + (c_6)_j \delta \theta_{j-1} \\ & + (c_7)_j \delta q_j + (c_8)_j \delta q_{j-1} = (r_7)_j, \end{aligned}$$

where $(a_1)_j = \frac{1}{2}v_{j-1/2} = (a_2)_j$, $(a_3)_j = -(u_{j-1/2} + \frac{M}{2}) = (a_4)_j$, $(a_5)_j = \frac{(1+K)}{h_j} + \frac{1}{2}f_{j-1/2}$, $(a_6)_j = -\frac{(1+K)}{h_j} + \frac{1}{2}f_{j-1/2}$, $(a_7)_j = \frac{K}{2} = (a_8)_j$, $(a_9)_j = \frac{\lambda}{2} = (a_{10})_j$, $(b_1)_j = \frac{1}{2}g_{j-1/2} = (b_2)_j$, $(b_3)_j = -\frac{1}{2}p_{j-1/2} = (b_4)_j$, $(b_5)_j = -\frac{K}{2} = (b_6)_j$, $(b_7)_j = -(\frac{u_{j-1/2}}{2} + K) = (b_8)_j$, $(b_9)_j = \frac{1}{h_j}(1 + \frac{K}{2}) + \frac{1}{2}f_{j-1/2}$, $(b_{10})_j = -\frac{1}{h_j}(1 + \frac{K}{2}) + \frac{1}{2}f_{j-1/2}$, $(c_1)_j = \frac{1}{2}q_{j-1/2} = (c_2)_j$, $(c_3)_j = -\frac{1}{2}\theta_{j-1/2} = (c_4)_j$, $(c_5)_j = -\frac{1}{2}u_{j-1/2} = (c_6)_j$, $(c_7)_j = \frac{1}{h_j P_r}(1 + \frac{4}{3F}) + \frac{1}{2}f_{j-1/2}$, $(c_8)_j = -\frac{1}{h_j P_r}(1 + \frac{4}{3F}) + \frac{1}{2}f_{j-1/2}$, $(r_1)_j = f_{j-1} - f_j + h_j u_{j-1/2}$, $(r_2)_j = u_{j-1} - u_j + h_j v_{j-1/2}$, $(r_3)_j = p_{j-1} - p_j + h_j g_{j-1/2}$, $(r_4)_j = \theta_{j-1} - \theta_j + h_j q_{j-1/2}$, $(r_5)_j = -\frac{(1+K)}{h_j}(v_j - v_{j-1}) - f_{j-1/2}v_{j-1/2} - (1+M) + (u_{j-1/2})^2 - Kg_{j-1/2} + Mu_{j-1/2} - \lambda\theta_{j-1/2}$, $(r_6)_j = -\frac{(1+K)}{h_j}(g_j - g_{j-1}) - g_{j-1/2}f_{j-1/2} + u_{j-1/2}p_{j-1/2} + 2Kp_{j-1/2} + Kv_{j-1/2}$, $(r_7)_j = -\frac{1}{P_r h_j}(1 + \frac{4}{3F})(q_j - q_{j-1}) - f_{j-1/2}q_{j-1/2} + u_{j-1/2}\theta_{j-1/2}$.

For all iterates, we take

$$(47) \quad \begin{aligned} \delta f_0 = 0, \quad \delta u_0 = 0, \quad \delta p_0 = 0, \quad \delta q_0 = 0, \\ \delta u_J = 0, \quad \delta p_J = 0, \quad \delta \theta_J = 0. \end{aligned}$$

3.3. The Block tridiagonal matrix. The linearised difference system (40) to (46) has a block tridiagonal structure as follows:

$$\begin{bmatrix} [A_1] & [C_1] & & & & & \\ [B_2] & [A_2] & [C_2] & & & & \\ & & & \dots & & & \\ & & & [B_{J-1}] & [A_{J-1}] & [C_{J-1}] & \\ & & & & [B_J] & [A_J] & \end{bmatrix} \begin{bmatrix} [\delta_1] \\ [\delta_2] \\ \dots \\ [\delta_{J-1}] \\ [\delta_J] \end{bmatrix} = \begin{bmatrix} [r_1] \\ [r_2] \\ \dots \\ [r_{J-1}] \\ [r_J] \end{bmatrix}$$

or,

$$(48) \quad \mathbf{A}\delta = \mathbf{r},$$

where

$$\begin{aligned} [A_1] &= \begin{bmatrix} 0 & 0 & 0 & 1 & 0 & 0 & 0 \\ d & 0 & 0 & 0 & d & 0 & 0 \\ 0 & d & 0 & 0 & 0 & d & 0 \\ 0 & 0 & -1 & 0 & 0 & 0 & d \\ (a_6)_1 & (a_8)_1 & (a_{10})_1 & (a_1)_1 & (a_5)_1 & (a_7)_1 & 0 \\ (b_6)_1 & (b_{10})_1 & 0 & (b_1)_1 & (b_5)_1 & (b_9)_1 & 0 \\ 0 & 0 & (c_6)_1 & (c_1)_1 & 0 & 0 & (c_7)_1 \end{bmatrix}, \\ [A_j] &= \begin{bmatrix} d & 0 & 0 & 1 & 0 & 0 & 0 \\ -1 & 0 & 0 & 0 & d & 0 & 0 \\ 0 & -1 & 0 & 0 & 0 & d & 0 \\ 0 & 0 & -1 & 0 & 0 & 0 & d \\ (a_4)_j & 0 & (a_{10})_j & (a_1)_j & (a_5)_j & (a_7)_j & 0 \\ (b_4)_j & (b_8)_j & 0 & (b_1)_j & (b_5)_j & (b_9)_j & 0 \\ (c_4)_j & 0 & (c_6)_j & (c_1)_j & 0 & 0 & (c_7)_j \end{bmatrix}, \\ & 2 \leq j \leq J; \end{aligned}$$

$$[B_j] = \begin{bmatrix} 0 & 0 & 0 & -1 & 0 & 0 & 0 \\ 0 & 0 & 0 & 0 & d & 0 & 0 \\ 0 & 0 & 0 & 0 & 0 & d & 0 \\ 0 & 0 & 0 & 0 & 0 & 0 & d \\ 0 & 0 & 0 & (a_2)_j & (a_6)_j & (a_8)_j & 0 \\ 0 & 0 & 0 & (b_2)_j & (b_6)_j & (b_{10})_j & 0 \\ 0 & 0 & 0 & (c_2)_j & 0 & 0 & (c_8)_j \end{bmatrix},$$

$$2 \leq j \leq J;$$

$$[C_j] = \begin{bmatrix} d & 0 & 0 & 0 & 0 & 0 & 0 \\ 1 & 0 & 0 & 0 & 0 & 0 & 0 \\ 0 & 1 & 0 & 0 & 0 & 0 & 0 \\ 0 & 0 & 1 & 0 & 0 & 0 & 0 \\ (a_3)_j & 0 & (a_9)_j & 0 & 0 & 0 & 0 \\ (b_3)_j & (b_7)_j & 0 & 0 & 0 & 0 & 0 \\ (c_3)_j & 0 & (c_5)_j & 0 & 0 & 0 & 0 \end{bmatrix},$$

$$1 \leq j \leq J-1.$$

Here $d = -\frac{h_j}{2}$,

$$[\delta_1] = \begin{bmatrix} \delta v_0 \\ \delta g_0 \\ \delta \theta_0 \\ \delta f_1 \\ \delta v_1 \\ \delta g_1 \\ \delta q_1 \end{bmatrix}, \quad [\delta_j] = \begin{bmatrix} \delta u_{j-1} \\ \delta p_{j-1} \\ \delta \theta_{j-1} \\ \delta f_j \\ \delta v_j \\ \delta g_j \\ \delta q_j \end{bmatrix}, \quad 2 \leq j \leq J;$$

$$[r_j] = \begin{bmatrix} (r_1)_j \\ (r_2)_j \\ (r_3)_j \\ (r_4)_j \\ (r_5)_j \\ (r_6)_j \\ (r_7)_j \end{bmatrix}, \quad 1 \leq j \leq J.$$

Forward sweep:

To solve equation (48), assume the matrix \mathbf{A} to be nonsingular and it can be factored as

$$(49) \quad \mathbf{A} = \mathbf{LU},$$

where

$$L = \begin{bmatrix} [\alpha_1] & & & & & & \\ [B_2] & [\alpha_2] & & & & & \\ & & \cdots & \cdots & & & \\ & & & [\alpha_{J-1}] & & & \\ & & & [B_J] & [\alpha_J] & & \end{bmatrix},$$

$$U = \begin{bmatrix} I & [\Gamma_1] & & & & & \\ & I & [\Gamma_2] & & & & \\ & & \cdots & \cdots & & & \\ & & & I & [\Gamma_{J-1}] & & \\ & & & & I & & \end{bmatrix},$$

$[I]$ is the identity matrix of order 7, and $[\alpha_j], [\Gamma_j]$ are 7×7 matrices whose elements are determined by the following equations:

$$(50) \quad [\alpha_1] = [A_1],$$

$$(51) \quad [A_1][\Gamma_1] = [C_1],$$

$$(52) \quad [\alpha_j] = [A_j] - [B_j][\Gamma_{j-1}], j = 2, 3, \dots, J,$$

$$(53) \quad [\alpha_j][\Gamma_j] = [C_j], j = 2, 3, \dots, J - 1.$$

Backward sweep:

Equation (49) can now be substituted in (48) and we get

$$(54) \quad \mathbf{LU}\delta = \mathbf{r},$$

Let

$$(55) \quad \mathbf{U}\delta = \mathbf{w},$$

Then the equation (54) becomes

$$(56) \quad \mathbf{Lw} = \mathbf{r},$$

where

$$\mathbf{w} = \begin{bmatrix} [w_1] \\ [w_2] \\ \cdots \\ [w_{J-1}] \\ [w_J] \end{bmatrix},$$

and the $[w_j]$ are 7×1 column matrices. The elements \mathbf{w} can be solved from the equation (56) by

$$(57) \quad [\alpha_1][w_1] = [r_1],$$

$$(58) \quad [\alpha_j][w_j] = [r_j] - [B_j][w_{j-1}], 2 \leq j \leq J.$$

With these $[w_j]$ and from equation (55) we get $[\delta_j]$:

$$(59) \quad [\delta_J] = [w_J],$$

$$(60) \quad [\delta_j] = [w_j] - [\Gamma_j][\delta_{j+1}], 1 \leq j \leq J - 1.$$

These iterations will be stopped when

$$(61) \quad |\delta v_0^{(i)}| < \varepsilon,$$

where ε is the desired level of accuracy.

4. Numerical Results and Discussions

With the help of the implicit finite-difference scheme known as the Keller-box method the equations (13), (14) and (15) subject to the boundary conditions (16),(17) are solved numerically. The step size $\Delta\eta$ of η and the edge of the boundary layer η_∞ had to be adjusted for different values of parameters to maintain accuracy within the interval $0 \leq \eta \leq \eta_\infty$, where η_∞ is the boundary layer thickness, we run the programme in MATLAB upto the desired level of accuracy. The validity of the numerical results has been compared with the results of Bachok and Ishak [2009] and they are found to be in a very good agreement, as presented in Table 1, when $\lambda = 1, K = 0, n = 0.5, M = 0, e = 0, s = 0$, $\Delta\eta = 0.02$ and $F = 7000$. The choice of $\eta_{max} = 15$ ensured that all numerical solutions approached the far field asymptotic values correctly. This is an important point that is often overlooked in publications on boundary layer flows (Pantokratotars [64]).

TABLE 1. Values of $f''(0)$ and $1/\theta(0)$ for different values of P_r

P_r	Bachok and Ishak (2009)		Present result	
	$f''(0)$	$1/\theta(0)$	$f''(0)$	$1/\theta(0)$
0.7	1.8339	0.7776	1.8339	0.7776
1.0	1.7338	0.8781	1.7339	0.8781
7.0	1.4037	1.6913	1.4037	1.6916
10.0	1.3711	1.9067	1.3711	1.9072

The variation of skin friction coefficient $f''(0)$ and the local Nusselt number $1/\theta(0)$ with λ for different values of the suction parameter s , the magnetic parameter M and the material parameter K are given by figures 3 to 6 respectively.

The dual solutions were obtained by setting two different values of η_∞ , which produce two different velocity and temperature profiles both satisfy the boundary conditions. It is seen that for the opposing flow ($\lambda < 0$) dual solutions are found

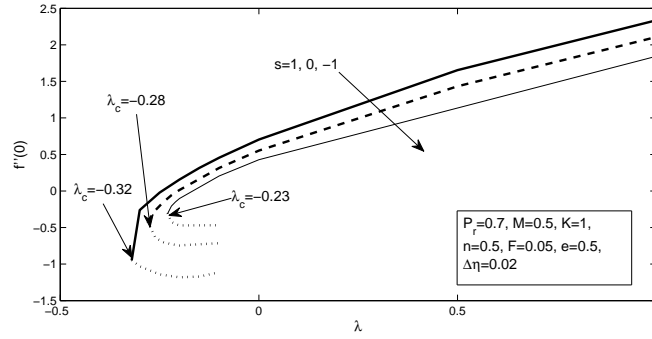


FIGURE 3. skin friction coefficient with s

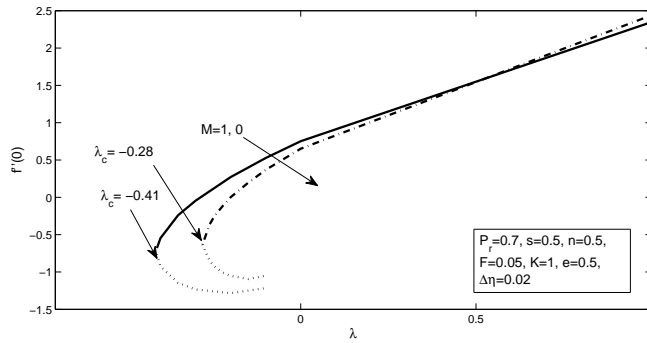


FIGURE 4. skin friction coefficient with M

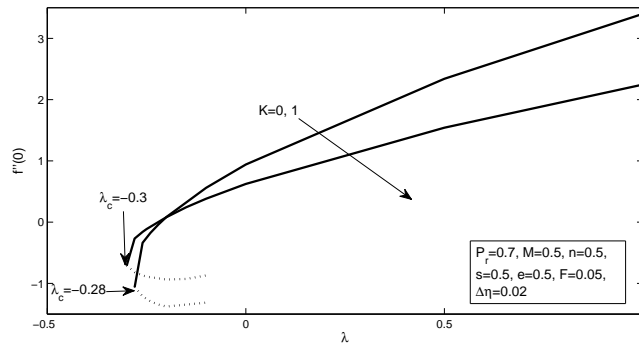


FIGURE 5. skin friction coefficient with K

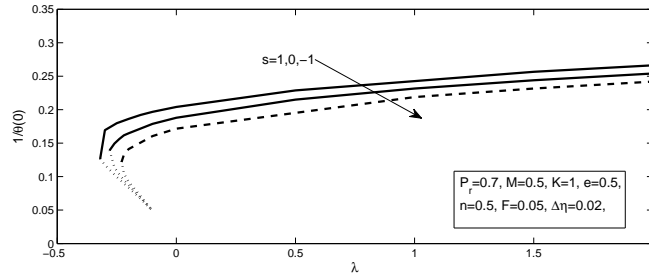


FIGURE 6. Local Nusselt number with s

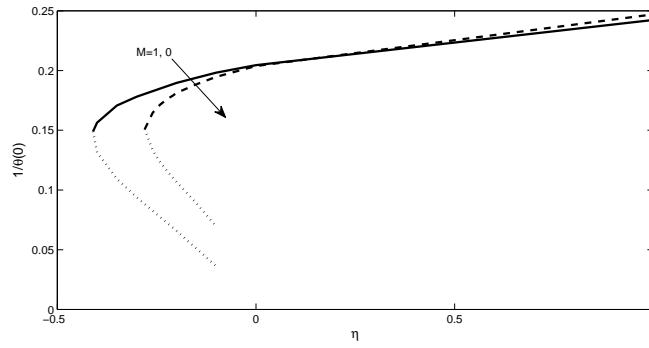


FIGURE 7. Local Nusselt number with M

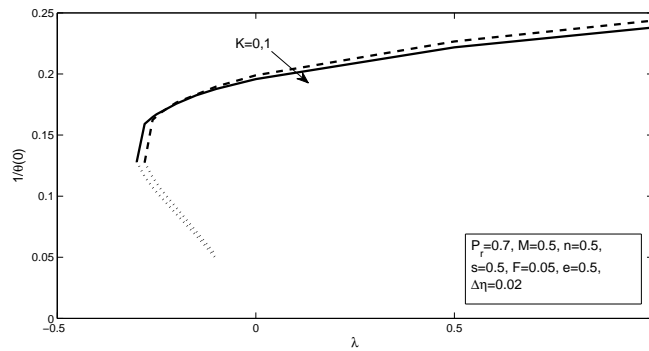


FIGURE 8. Local Nusselt number with K

to exist for the values of s , M and K considered. For a particular value of s , M and K the solution is present up to a critical value of λ , say λ_c , outside which the boundary layer separates from the surface and the solution based upon the

boundary-layer approximations are not feasible. It is clear from the figures 3 to 8 that larger values of s , M and K enhance the range of λ for which the solution exists. In this study the critical values of λ (i.e., λ_c) are given by the Table 2.

TABLE 2. Critical values of λ (i.e., λ_c)

	s			M		K	
	-1	0	1	0	1	0	1
λ_c	-0.23	-0.28	-0.32	-0.28	-0.41	-0.28	-0.30

Hence the boundary-layer separation is delayed with increase of s , M and K . So suction and Magnetic field holdup the boundary layer separation respectively compared to the no-suction ($s = 0$) and non-magnetic field ($M = 0$) case. Similarly micropolar fluids ($K \neq 0$) delay the boundary-layer separation as compared to the classical Newtonian fluids ($K = 0$). Figures 3, 4 and 5 respectively depict that the value of $|f''(0)|$ decreases as s , M and K increase, thus suction, magnetic field and micropolar fluids show drag reduction compared to the non-suction, non-magnetic field and classical Newtonian fluids respectively.

Figures 9–17 display the dual solutions for the opposing flow for different values of s , K and M where the first solutions are stable with the most physical relevance while the second solutions are not. The region of reversed flow exists for the case of the second solutions from figures 9, 10 and 11 and this would be unacceptable as possible asymptotic solutions to which a fully forward flow developing near the stagnation point could grow.

The velocity, angular velocity and temperature profiles for both assisting ($\lambda > 0$) and opposing flow ($\lambda < 0$) are given in the figures 9 to 17 for different values of the suction parameter s , K and M respectively. Here $P_r = 0.7$, $n = 0.5$, $e = 0.5$, $s = 0.5$, $M = 0.5$, $K = 1.0$ and $F = 0.05$.

Figures 9 and 10 depict that the velocity profiles decrease for the assisting flow and for the opposing flow (second solution) but the profile increases for the opposing flow (first solution) with the increase of s and M respectively. Figure 11 describes that the velocity profiles decrease with the increase of K for the both flows.

For the assisting flow angular velocity profiles increase near boundary but after a certain point the profiles decrease with the increasing of s and for the opposing flows (first and second solution) the profiles decrease with s (fig. 12). Figure 14 shows that the angular velocity profiles decrease near boundary but increase after some η with the increase of K for the assisting flow, the reverse result holds for the opposing flow (second solution) and the profiles decrease with K for the opposing flow (first solution). Figure 13 describes that the angular velocity profiles increase near boundary but the profiles decrease with the increasing of M for the assisting flow and for the opposing flow (second solution) after some distance from the boundary and the reverse result holds for the opposing flow (first solution).

From the figure 15 it is clear that the temperature profiles decrease with the increase of s for the assisting flow and for the opposing flow (first solution) but

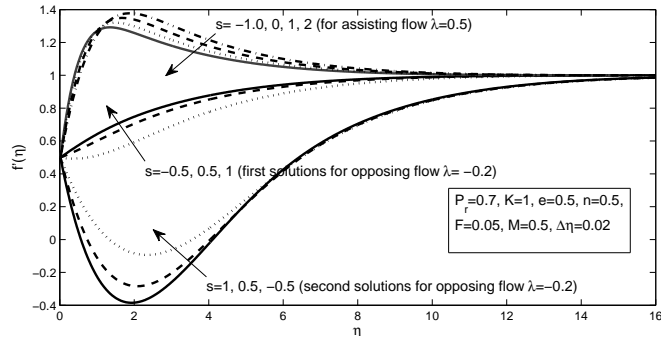


FIGURE 9. Velocity profile for different s

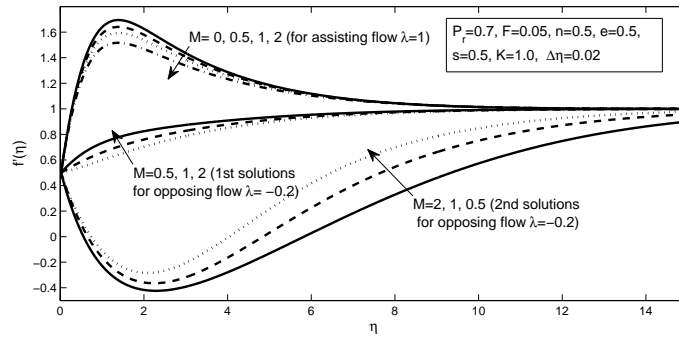


FIGURE 10. Velocity profiles for different M

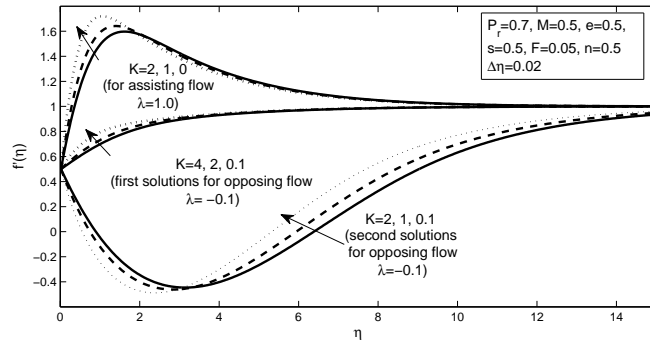


FIGURE 11. Velocity profiles for different K

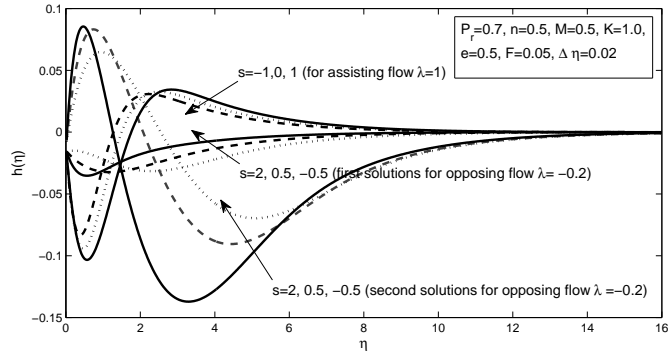


FIGURE 12. Angular velocity profile for different s

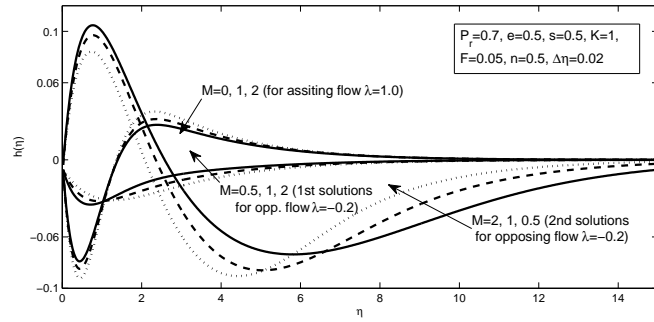


FIGURE 13. Angular velocity profiles for different M

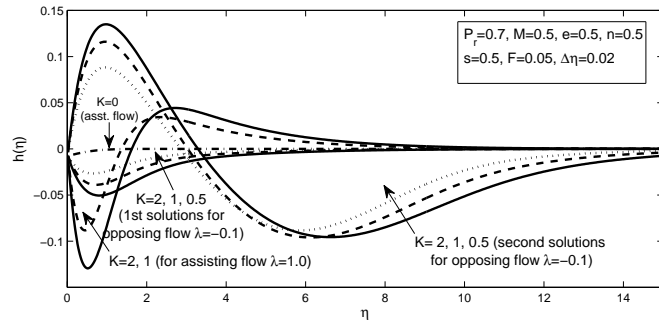


FIGURE 14. Angular velocity profiles for different K

increase for the opposing flow (second solution). The profiles enhance with the increase of K for both the flows (Figure 17). For the assisting flow the temperature profiles increase with M , but the reverse result holds for the opposing flow (Figure 16).

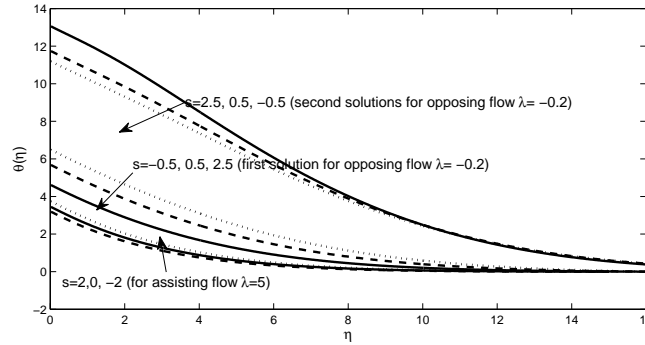


FIGURE 15. Temperature profiles for different s

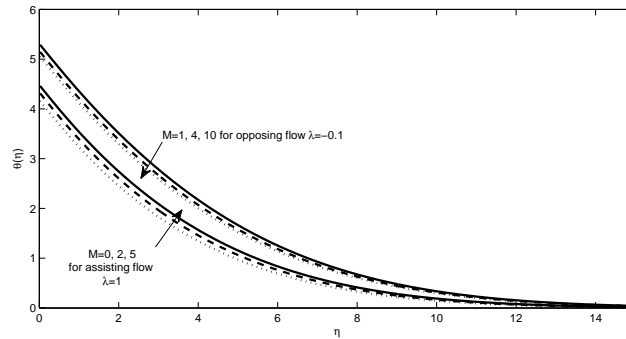
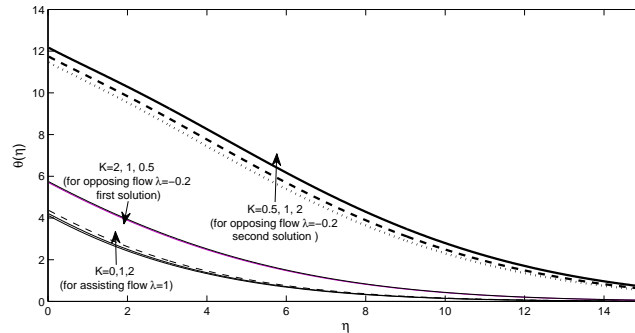


FIGURE 16. Temperature profiles for different M

5. Conclusions

A numerical study is performed for the problem of the steady laminar mixed convection boundary layer flow on a vertical surface under prescribed heat flux. The velocity, angular velocity and temperature profiles are affected by the suction parameter, magnetic parameter, material parameter, Prandtl number and the buoyancy parameter for both assisting and opposing flows. The following observations are made:

FIGURE 17. Temperature profiles for different K

- I Suction, magnetic field and micropolar fluids delay the boundary-layer separation as well as show drag reduction as compared to the non-suction, non-magnetic field and the classical Newtonian fluids respectively.
- II Dual similarity solutions are found to exist for the opposing flow, while for the assisting flow, the solution is unique. The first solutions are stable with the most physical relevance while the second solutions are not.
- III Velocity profiles decrease for the assisting flow with the increase of s , M , K . The profiles increase with the increase of the suction parameter and the magnetic parameter but decrease with the increase of material parameter for the opposing flow (first solution).
- IV For the assisting flow the angular velocity profiles increase near boundary but after a certain point the profiles decrease with the increasing of the suction parameter and the magnetic parameter but the reverse holds with the enhance of the material parameter. For the opposing flow (first solution) the profiles decrease with the increase of s , K , but with the increase of M the profiles decrease near boundary and then increase.
- V For the assisting flow the temperature profiles decrease with the increase of suction parameter but increase with the increase of the material parameter and the magnetic parameter. The profiles decrease with s and M but almost no change with K for the opposing flow (first solution).

References

- [1] T.R. Mahapatra and A.G. Gupta, *Heat transfer in stagnation point flow towards a stretching sheet*, Heat Mass Transfer, **38** (2002), 517-521.
- [2] C.Y. Wang, *Stagnation point flow towards a shrinking sheet*, Int. J. Non-Linear Mech., **43** (2008), 377-382.
- [3] Y.Y. Lok, N. Amin and I. Pop, *Non-orthogonal stagnation point flow towards a stretching sheet*, Int. J. Non-Linear Mech., **41** (2006), 622-627.
- [4] B.C. Sakiadis, *Boundary-layer behavior on continuous solid surfaces: I Boundary-layer equations for two dimensional and axisymmetric flow*, AICHE J. **7** (1961), 26-28.

- [5] B.C.Sakiadis, *Boundary-layer behavior on continuous solid surfaces: II The Boundary-layer on a continuous flat surface*, AICHE J., **7** (1961), 221-225.
- [6] B.C.Sakiadis, *Boundary-layer behavior on continuous solid surfaces: III The Boundary-layer on a continuous cylindrical surface*, AICHE J., **7** (1961), 467-472.
- [7] L.J.Grubka and K.M. Bobba, *Heat transfer characteristics of a continuous stretching surface with variable temperature*, Trans. ASME J. Heat Transfer, **107** (1985), 248-250.
- [8] R.Cortell, *Effects of viscous dissipation and radiation on the thermal boundary layer over a nonlinearly stretching sheet*, Phys.Lett.A, **372** (2008), 631-636.
- [9] J.R. Spreiter and A.W. Rizzi, *Aligned magnetohydrodynamic solution for solar wind flow past the earth's magnetosphere*, Acta Astronaut. **1(1-2)** (1974), 15-35.
- [10] O.Nath, S.N.Ojha and H.S. Takhar, *A study of stellar point explosion in a radiative magnetohydrodynamic medium*, Astrophys. Space Sci. **183** (1991), 135-145.
- [11] T.M.Chen, *Radiation effects on magnetohydrodynamic free convection flow*, AIAA J. Thermophys. Heat Transfer, **22 (10)** (2008), 125-128.
- [12] N.F.M. Noor, S.Abbasbandy and I. Hashim, *Heat and mass transfer of thermophoretic MHD flow over an inclined radiative isothermal permeable surface in the presence of heat source/sink*, Int. J. Heat Mass Transfer, **55** (2012), 2122-2128.
- [13] A. Aziz, *A similarity solution for laminar thermal boundary layer over a flat plate with a convective surface boundary condition*, Commun. Nonlinear Sci. Numer. Simul., **14 (4)** (2009), 1064-1068.
- [14] R.C. Bataller, *Radiation effects for the Blasius and Sakiadis flows with a convective surface boundary condition*, Appl.Math. Comput., **206** (2008), 832-840.
- [15] O.D. Makinde, *Similarity solution of hydromagnetic heat and mass transfer over a vertical plate with a convective surface boundary condition*, Int. J. Phys. Sci., **5(6)** (2010), 700-710.
- [16] O.D. Makinde, *On MHD heat and mass transfer over a moving vertical plate with a convective surface boundary condition*, Can. J. Chem. Eng., **88** (2010), 983-990.
- [17] A.C. Eringen, *Theory of Micropolar Fluids*, J. Math. Mech., **16** (1966), 1-18.
- [18] A.C. Eringen, *Theory of Thermomicropolar Fluids*, J. Math. Appl., **38** (1972), 480-495.
- [19] M.M. Khonsari, *On the self-excited whirl orbits of a journal in a sleeve bearing lubricated with micropolar fluids*, Acta Mech., **81** (1990), 235-244.
- [20] B. Hadimoto and T. Tokioka, *Two-dimensional shear flows of linear micropolar fluids*, Int. J. Eng. Sci., **7** (1969), 515-522.
- [21] J.D. Lee and A.C. Eringen, *Boundary effects of orientation of nematic liquid crystals*, J. Chem. Phys., **55** (1971), 4509-4512.
- [22] T. Ariman, M.A. Turk and N.D. Sylvester, *Application of Microcontinuum fluid mechanics*, Int. J. Eng. Sci., **12** (1974), 273-293.
- [23] V. Kolpashchikov, N.P. Migun and P.P. Prokhorenko, *Experimental determinations of material micropolar coefficients*, Int. J. Eng. Sci. **21** (1983), 405-411.
- [24] T. Ariman, M.A. Turk and N.D. Sylvester, *Microcontinuum fluid mechanics- review*, Int. J. Eng. Sci., **11** (1974), 905-930.
- [25] Yucel A., *Mixed convection in micropolar fluid flow over a horizontal plate with surface mass transfer*, Int. J. Eng. Sci., **27** (1989), 1593-1602.
- [26] S.K. Jena and M.N. Mathur, *Similarity solution for laminar free convection flow of thermomicropolar fluid past a non-isothermal vertical flat plate*, Int. J. Eng. Sci., **19** (1981) 1431-1439.
- [27] R.S.R. Gorla, *Combined forced and free convection in micropolar boundary layer flow on a vertical flat plate*, Int. J. Eng. Sci., **26** (1983), 385-391.
- [28] M.A. Hossain, M.K. Chowdhury and H.S. Takhar, *Mixed convection flow of micropolar fluids with variable spin gradient viscosity along a vertical plate*, J. Theo. Appl. Fluid Mech., **1** (1995), 64-77.
- [29] Y. Mori, *Buoyancy effects in forced laminar convection flow over a horizontal flat plate*, J. Heat transfer, **83** (1961), 479-482.
- [30] G. Lukaszewicz, *Micropolar fluids: theory and application*, (1999) (Birkhuser, Basel).

- [31] A.C. Eringen , *Microcontinuum field theories, II. Fluent Media*, (2001) (Springer, New York).
- [32] R. Nazar, N. Amine, D. Filip and I.Pop, *Stagnation point flow of a micropolar fluid towards a stretching sheet*, Int. J. Non-Linear Mech., **39** (2004), 1227-1235.
- [33] A. Ishak, Y.Y. Lok and I.Pop, *Stagnation point flow over a shrinking sheet in a micropolar fluid*, Chem. Eng. Commun., **197** (2010), 1417-1427.
- [34] A. Ishak , R. Nazar and I. Pop, *Mixed convection stagnation point flow of a micropolar fluid towards a stretching sheet* , Mechanica, **43** (2008), 411-418.
- [35] T. Hayat, T. Javed and Z. Abbas, *MHD flow of a micropolar fluid near a stagnation-point towards a non-linear stretching surface*, Non-Linear Analysis: Real World Applications, **10** (2009) ,1514-1526.
- [36] S. Nadeem, M.Hussani and M.Naz, *MHD stagnation flow of a micropolar fluid through a porous medium* , Mechanica, **45** (2010), 869-880.
- [37] M. Ashraf, M.M. Ashraf, *MHD stagnation point flow of a micropolar fluid towards a heated surface*, Appl. Math. Mech - Engl. Ed., **32(1)** (2011), 45-54.
- [38] F.M. Ali, R.Nazar, N.M. Arifin, I.Pop, *MHD stagnation-point flow and heat transfer towards strching sheet with induced magnetic field*, Appl. Math. Mech.-Engl. Ed., **32(4)** (2011),409-418.
- [39] T. Hayat, A. Rafique, M.Y. Malik, S. Obaidat, *Stagnation-point flow of Maxwell fluid with magnetic field and radiation effects*, Heat transfer- Asian Research, **41(1)** (2012), 23-32.
- [40] N. Ramachandran, T.S. Chen and B.F. Armaly, *Mixed convection in stagnation flows adjacent to a vertical surfaces*, ASME Jr. Heat Transfer, **110** (1988), 373-377.
- [41] C.D.S. Devi, H.S. Takhar and G. Nath, *Unsteady mixed convection flow in stagnation region adjacent to a vertical surface*, Int. J. Heat Mass Transfer, **26** (1991), 71-79.
- [42] Y.Y. Lok, N.Amin, D. Campean and I. Pop , *Steady mixed convection flow of a micropolar fluid near the stagnation point on a vertical surface*, Int. J. Num. Methods Heat Fluid Flow, **15** (2005), 654-670.
- [43] T.R. Mahapatra and A.S. Gupta, *Magnetohydrodynamic stagnation point flow towards a stretching sheet*, Acta Mech., **152** (2001), 191-196.
- [44] C.H. Chen, *Combined effects of Joule heating and viscous dissipation on Magnetohydrodynamic flow past a permeable stretching surface with free convection and radiative heat transfer*, ASME J. Heat transfer, **132** (2010), P064503.
- [45] K.E. Chin, R. Nazar, N. Arifin and I. Pop, *Effect of variable viscosity on mixed convection boundary layer flow over a vertical surface embedded in a porous medium*, Int. Commun. Heat Mass Transfer, **34** (2007), 464-473.
- [46] S.C. Ling, R. Nazar and I. Pop , *Steady mixed convection boundary layer flow over a vertical flat plate in a porous medium filled with water at 40C: case of variable wall Temperature*, Trans. Porous Med., **69** (2007), 359-372.
- [47] A. Ishak , R. Nazar and I. Pop, *Magnetohydrodynamic stagnation point flow towards a stretching vertical sheet in a micropolar fluid*, Magnetohydrodynamic, **43** (2007), 83-97.
- [48] K. Das, *Hydromagnetic thermal boundary layer flow of a perfectly conducting fluid*, Turk Jr. Phy., **35** (2011), 161-171.
- [49] S. Mukhopadhyay, S. Uddin and G.C. Layek , *Lie group analysis of MHD boundary layer slip flow past a heated stretching sheet in presence of Heat source/sink*, Int. J. Appl. Math. and Mech., **8(16)** (2012), 51-66.
- [50] G.C. Shit and R. Halder, *Thermal radiation effects on MHD viscoelastic fluid flow over a stretching sheet with variable viscosity*, Int. J. of Appl. Math. and Mech., **8(14)** (2012), 14-36.
- [51] A. Adhikari and D.C. Sanyal, *Heat transfer on MHD viscous flow over a stretching sheet with prescribed heat flux*, Bull. Int. Math. Virtual Instt., **3** (2013), 35-47.
- [52] A.Adhikari, *MHD micropolar fluid flowtowards a stagnation point on a vertical surface under induced magnetic field with radiative heat flux*, Int. J. of Engg. Research and Tech., **2(8)** (2013), 135-144.

- [53] K.R. Cramer *Several Magnetohydrodynamic free convection solutions*, ASME J. Heat Transfer, **85** (1963), 35-40.
- [54] M.H. Cobble, *Free convection with mass transfer under the influence of a magnetic field*, Nonlinear Anal. Theo. Methods Appl., **3** (1979), 135-143.
- [55] A. Raptis, C. Perdikis and G. Tziranidis, *Effects of free convection currents on the flow of an electrically conducting fluid past an accelerated vertical infinite plate with variable suction*, J. Appl. Mech., **61** (1981), 341-342.
- [56] M. Kumari, A. Slaouti, H.S. Takhar, S. Nakamura and G. Nath, *Unsteady free convection flow over a continuous moving vertical surface*, Acta Mech., **116** (1996), 75-82.
- [57] N. Bachok and A. Ishak, *MHD stagnation-point flow of a Micropolar Fluid with Prescribed Wall Heat Flux*, European J. of Sci. Research, **35(3)** (2009), 436-443.
- [58] G. Ahmadi, *Self-similar solution of incompressible micropolar boundary layer flow over a semi-infinite flat plate*, Int. J. Eng. Sci., **14** (1976), 639-646.
- [59] M.Q. Brewster, *Thermal Radiative Transfer Properties*, John Wiley and Sons, Canada, 1992.
- [60] D.A.S. Rees and A.P. Bassom, *The Blasius boundary-layer flow of a micropolar fluid*, Int. J. Eng. Sci., **34** (1996), 113-124.
- [61] T. Cebeci and P. Bradshaw, *Physical and Computational Aspects Convective Heat Transfer*, (1988) (Springer, New York).
- [62] T. Cebeci and J. Cousteix, *Modeling and Computing of Boundary-Layer Flows : Laminar, Turbulent and Transitional Boundary Layers in Incompressible and Compressible Flows*, (2005) (Springer).
- [63] T.Y. Na, *Computational Methods in Engineering Boundary Value Problem*, (1979) (Academic Press).
- [64] A. Pantokratoras, *Study of MHD boundary layer flow over a heated stretching sheet with variable viscosity: a numerical reinvestigation*, Int. J. Heat Mass Transfer, **51** (2008), 104-110.

Received 01.01.2014. Revised 10.04.2014. available online 01.12.2014.

DEPARTMENT OF MATHEMATICS, SHYAMPUR SIDDHESWARI MAHAVIDYALAYA, AJODHYA, HOWRAH-711312, WEST BENGAL, INDIA

E-mail address: adhikarianimesh@gmail.com